EUROPEAN LABORATORY FOR PARTICLE PHYSICS

ADDENDUM TO THE NA61/SHINE PROPOSAL SPSC-P-330

Hadron Production Measurements for Fermilab Neutrino Beams

October 14, 2014

http://na61.web.cern.ch/

Abstract

An extension of the NA61/SHINE physics program utilizing hadron production measurements for Fermilab neutrino beams is proposed. The initiative originated from the US groups (the US-NA61 Collaboration) and is supported by the NA61/SHINE Collaboration. The US groups intend to join the NA61/SHINE Collaboration to perform these measurements. We wish to collect dedicated and optimized high-precision hadron production data needed for improved neutrino beams modeling necessary for ongoing and future experiments at Fermilab. Presented is a schedule, analysis and a detector upgrade plan to expose thin targets and replicas of targets used at Fermilab to the NA61/SHINE hadron beam to accumulate a suitably large sample of events to provide a data set which would be essential for future neutrino beams including running experiments using the NuMI and LBNF facilities.

The US-NA61 Collaboration

S. R. Johnson, A. Marino, E. D. Zimmerman

University of Colorado, Boulder, Colorado 80302, USA

D. Harris, A. Marchionni

Fermi National Accelerator Laboratory, Batavia, Illinois 60510, USA

C. Mauger, G. B. Mills*

Los Alamos National Laboratory, Los Alamos, New Mexico 87545, USA

N. Graf, B. Messerly, D. Naples, V. Paolone

Department of Physics and Astronomy, University of Pittsburgh, Pittsburgh, Pennsylvania 15260, USA

T. Carroll, K. Lang

Department of Physics, University of Texas at Austin, Austin, Texas 78712, USA

L. Aliaga, M. Kordosky, J. Nelson

Department of Physics, College of William & Mary, Williamsburg, Virginia 23187, USA

* contact person

The NA61/SHINE Collaboration

N. Abgrall[17], A. Aduszkiewicz[22], Y. Ali[20], T. Antićić[2], N. Antoniou[7], B. Baatar[12], F. Bay[15], A. Blondel[17], J. Blümer[4], M. Bogomilov[1], A. Bravar[17], J. Brzychczyk[20], S.A. Bunyatov[12], O. Busygina[11], P. Christakoglou[7], T. Czopowicz[24], N. Davis[7], S. Debieux[17], H. Dembinski[4], F. Diakonos[7], S. Di Luise[15], W. Dominik[22], T. Drozhzhova[13], J. Dumarchez[3], K. Dynowski[24], R. Engel[4], A. Ereditato[16], G.A. Feofilov[13], Z. Fodor[8,23], A. Fulop[8], M. Gaździcki[6,18], M. Golubeva[11], K. Grebieszkow[24], A. Grzeszczuk[21], F. Guber[11], A. Haesler[17], T. Hasegawa[9], M. Hierholzer[16], R. Idczaki[23], S. Igolkin[13], A. Ivashkin[11], D. Joković[14], K. Kadija[2], A. Kapoyannis[7], E. Kaptur[21], D. Kiełczewska[22], M. Kirejczyk[22], J. Kisiel[21], T. Kiss[8], T. Kobayashi[9], P. Koevesarki[23], V.I. Kolesnikov[12], D. Kolev[1], V.P. Kondratiev[13], A. Korzenev[17], S. Kowalski[21], A. Krasnoperov[12], A. Kurepin[11], D. Larsen[20], A. László[8], V.V. Lyubushkin[12], M. Maćkowiak-Pawłowska[24,6], Z. Majka[20], B. Maksiak[24], A.I. Malakhov[12], A. Marcinek[20], V. Marin[11], K. Marton[8], H.-J. Mathes[4], T. Matulewicz[22], V. Matveev[11,12], G.L. Melkumov[12], S. Mrówczyński[18], S. Murphy[17], T. Nakadaira[9], M. Nirkko[16], K. Nishikawa[9], T. Palczewski[19], G. Pálla[8], A.D. Panagiotou[7], W. Peryt[24], O. Petukhov[11], C. Pistillo[16], R. Płaneta[20], J. Pluta[24], B.A. Popov[12], M. Posiadała[22], S. Puławski[21], J. Puzović[14], W. Rauch[5], M. Ravonel[17], A. Redij[16], R. Renfordt[6], E. Richter-Was[20], A. Robert[3], D. Röhrich[10], E. Rondio[19], M. Roth[4], A. Rubbia[15], A. Rustamov[6], M. Rybczynski[18], A. Sadovsky[11], K. Sakashita[9], K. Schmidt[21], T. Sekiguchi[9], P. Seyboth[18], D. Sgalaberna[15], M. Shibata[9], R. Sipos[8], E. Skrzypczak[22], M. Słodkowski[24], P. Staszel[20], G. Stefanek[18], J. Stepaniak[19], H. Stroebele[6], T. Šuša[2], M. Szuba[4], M. Tada[9], V. Tereshchenko[12], T. Tolyhi[8], R. Tsenov[1], L. Turko[23], R. Ulrich[4], M. Unger[4], M. Vassiliou[7], D. Veberič[4], V.V. Vechernin[13], G. Vesztergombi[8], L. Vinogradov[13], A. Wilczek[21], Z. Wlodarczyk[18], A. Wojtaszek[18], O. Wyszyński[20], L. Zambelli[3], and W. Zipper[21]

[1] Faculty of Physics, University of Sofia, Sofia, Bulgaria

[2] Ruđer Bošković Institute, Zagreb, Croatia

[3] LPNHE, University of Paris VI and VII, Paris, France

[4] Karlsruhe Institute of Technology, Karlsruhe, Germany

[5] Fachhochschule Frankfurt, Frankfurt, Germany

[6] University of Frankfurt, Frankfurt, Germany

[7] University of Athens, Athens, Greece

[8] Wigner Research Centre for Physics of the Hungarian Academy of Sciences, Budapest, Hungary

[9] Institute for Particle and Nuclear Studies, KEK, Tsukuba, Japan

[10] University of Bergen, Berge, Norway

[11] Institute for Nuclear Research, Moscow, Russia

[12] Joint Institute for Nuclear Research, Dubna, Russia

[13] St. Petersburg State University, St. Petersburg, Russia

[14] University of Belgrade, Belgrade, Serbia

[15] ETH Zürich, Zürich, Switzerland

[16] University of Bern, Bern, Switzerland

[17] University of Geneva, Geneva, Switzerland

[18] Jan Kochanowski University in Kielce, Poland

[19] National Center for Nuclear Research, Warsaw, Poland

[20] Jagiellonian University, Cracow, Poland

[21] University of Silesia, Katowice, Poland

[22] Faculty of Physics, University of Warsaw, Warsaw, Poland

[23] University of Wrocław, Wrocław, Poland

[24] Warsaw University of Technology, Warsaw, Poland

1 Introduction

The U.S. intensity frontier program in long-baseline neutrino physics is currently based on a number of active and planned neutrino experiments. Those include experiments at Fermilab's NuMI facility (Neutrinos from the Main Injector) such as MINERvA [1], MINOS+ [2], NOvA [3], and future long baseline neutrino experiments and facilities such as LBNE and LBNF. Those experiments all plan to use high-intensity proton beams from the Fermilab main injector, in the energy range 80-120 GeV that impinge upon graphite and/or beryllium targets. The subsequent pion and kaon secondaries are focused by aluminum horns and decay in flight to produce the neutrinos required by the experiments. A precise understanding of the neutrino flux from those beams is of paramount importance to the program.

Precise calculations of neutrino fluxes in such high-energy accelerator beams are limited at present by our knowledge of hadron production cross-sections in hadron-nucleus collisions. The modeling of strong-interaction cascades and hadronic yields from "thick" targets (up to a couple of interaction lengths) relies on detailed knowledge of underlying physics and cross-sections, which must be provided as a starting point to simulations. The resulting prediction of the flux of neutrinos, produced from decays of pions, kaons, and muons emerging from a hadronic shower and beamline re-interactions, is usually an essential part of simulations of most neutrino experiments. Knowledge of the neutrino flux is essential for experiments that measure neutrino cross sections. Two-detector neutrino oscillations experiments predict the neutrino flux at the far detector by using neutrino fluxes "calibrated" (or appropriately scaled) by event energy spectra measured in the near detector. However, even these experiments must rely on the beam simulations since the decay pipe (where most beam neutrinos are created) provides different angular acceptance for the two detectors. A timely opportunity to remedy this situation for the long-baseline NuMI beam at Fermilab, the future LBNE/LBNF long-baseline facility, and possibly other Fermilab beams is the subject of in this proposal.

The need for hadron production measurements may be particularly acute in the case of LBNE/LBNF. The LBNE/LBNF physics program requires an accurate determination of the

CP violating phase of the neutrino mixing matrix, which can only be accomplished with a precise prediction for the electron neutrino event rate in the far liquid argon detector. Without an identical liquid argon near detector, the systematic errors due to the liquid argon detector response will not cancel in a Far/Near event yield ratio, the technique used by the MINOS experiment, for example. A relatively small investment in this proposal would provide a significantly lower risk for the LBNE experiment's goals.

2 Overview of the US-NA61 Proposed Program

We wish to collect dedicated and optimized high-precision hadron production data needed for improved neutrino beams modeling necessary for ongoing and future experiments at Fermilab. Presented is a schedule, manpower, analysis and detector upgrade plan to expose thin targets and replicas of targets used at Fermilab to the NA61 hadron beam to accumulate a suitably large sample of events to provide a data set which would be essential for future neutrino beams including running experiments using the NuMI and LBNF facilities. The ideal experiment for our purposed is the NA61/SHINE experiment [12], shown in Figure 1.

2.1 Manpower

We expect the US effort required to expose thin targets and NuMI and LBNF target replicas in NA61/SHINE, and produce useful results, will ultimately require about 15 person-years of effort, that will include contributions to the NA61/SHINE common fund, hardware upgrades, simulations of NA61/SHINE detector configurations, which would be the most suitable for Fermilab beams, data taking, calibration, reconstruction, and analysis. In addition we wish to contribute to the NA61/SHINE detector upgrades that support these goals including the readout electronics and forward tracking upgrade. A survey of US institutions resulted in an estimate of committed manpower and is summarized in Tables 1 and 2 and shows that this requirement can be met with the present level of interest. The large majority of these FTE's would be paid for by redirecting existing operating budgets from the contributing institutions. In FY2015-18 funds for (averaged) three postdocs and four graduate

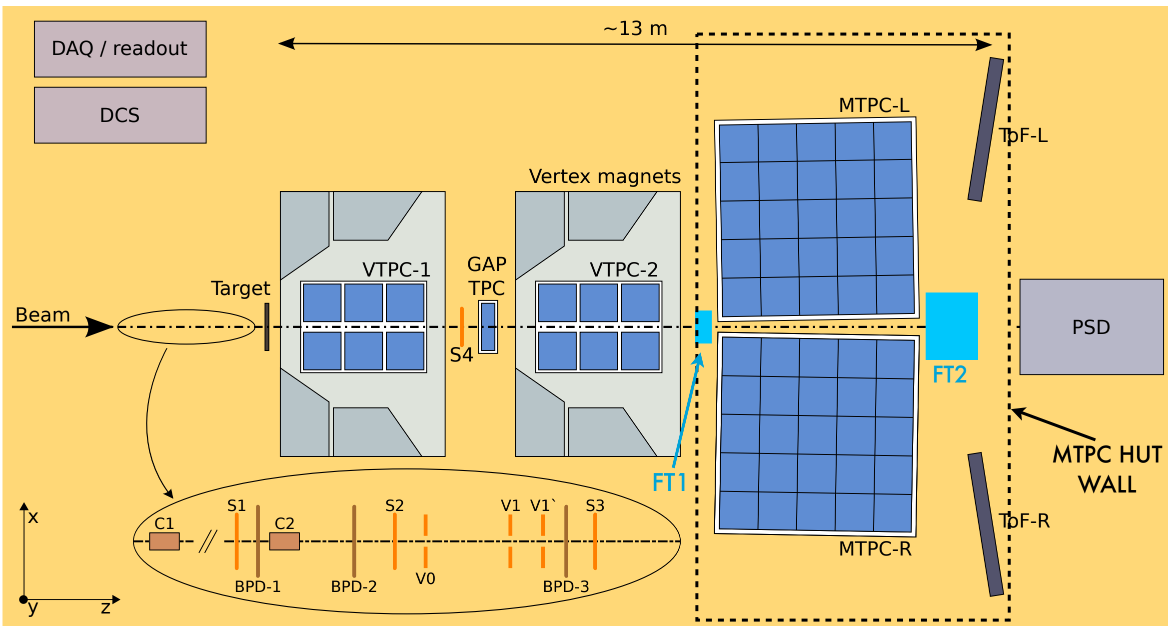

Figure 1: The NA61/SHINE experimental apparatus. The experiment is centered around two large dipole magnets, which can generate a combined 9 T-m of bending power. The magnet gaps and downstream area are filled with a large TPC system, which is in turn followed by a wall of ToF counters. The beam trigger is comprised of two Cherenkov counters C1/C2, two scintillator counters S1/S2, two veto counters (V0/V1, and three tracking chambers BPD1-3. The locations of the proposed forward tracking chambers (Sec. 6.2) are indicated as FT1 and FT2.

students per year would be needed.

	Senior Personnel (Fraction FTE/yr)	Post Docs (Fraction FTE/yr)	Graduate Students (Fraction FTE/yr)
FY2014	1.6	0.7	1.0
FY2015-18	2	2.5	3.7

Table 1: A summary of estimated US-NA61 staffing commitments.

Institution	Senior Personnel (Fraction FTE/yr)	Post Docs (Fraction FTE/yr)	Students (Fraction FTE/yr)
Los Alamos	0.25	0.5	0.2
University of Colorado	0.75	1	2
University of Pittsburgh	0.75	1	1
William and Mary	0.25	0	0.5

Table 2: Proposed US-NA61 staffing commitments by institution for FY2015-2018.

2.2 Contributions to Detector Upgrades

The proposed US hardware contributions to NA61/SHINE [12] are participation in the upgrade of the readout electronics and to instrument the far-forward region with two TPCs, one immediately upstream and one immediately downstream of the MTPCs. These chambers should have enough extent in the longitudinal direction to allow full tracking coverage, and π-proton separation, across the current gap that exists in the MTPC system. Details of the upgrades are given in subsequent sections.

3 Improving neutrino experiments at Fermilab

The new data will improve neutrino experiments at Fermilab and beyond. Results will enhance the modeling of all neutrino beams, primarily NuMI, BNB (Booster Neutrino Beam), and the proposed LBNE or LBNF. We also note that the neutrino experiments themselves, particularly those collecting large event samples, provide additional constraints on the flux simulations. However, they do not supply direct information on primary interactions.

Below we present brief comments on how improved beam simulation will impact the ongoing and upcoming Fermilab experiments.

3.1 MINERνA

MINERνA [1] is a dedicated neutrino-nucleus scattering experiment positioned just upstream of the MINOS near detector in the NuMI neutrino beam at Fermilab. The goal of the experiment is high-statistics, absolute measurements of inclusive and exclusive interaction rates for neutrinos and antineutrinos in the 1–20 GeV energy range. MINERνA makes use of a fine-grained, fully active detector design and a range of nuclear target materials (H_2O, He, C, Fe, Pb). By measuring rates on different atomic nuclei in the same detector and neutrino beam, MINERνA will study the effects of the dense nuclear medium on neutrino interactions.

As a neutrino cross section experiment, much of MINERνA's physics program is directly impacted by the accuracy of the neutrino flux determination, so dedicated hadron production data represents an important opportunity for the experiment. Also, the physics program of MINERνA is closely tied to the goals of future long-baseline neutrino oscillation experiments. Precision measurements of neutrino oscillation parameters, including the discovery of CP violation, will require detailed knowledge of inclusive and exclusive cross sections for both neutrinos and antineutrinos.

Figure 2 shows the region of phase space (in terms of momentum and polar angle) for secondary π's and K's that contribute to neutrino events in the MINERνA detector. There is a lot of overlap with the NA61 acceptance shown in Figure 3.

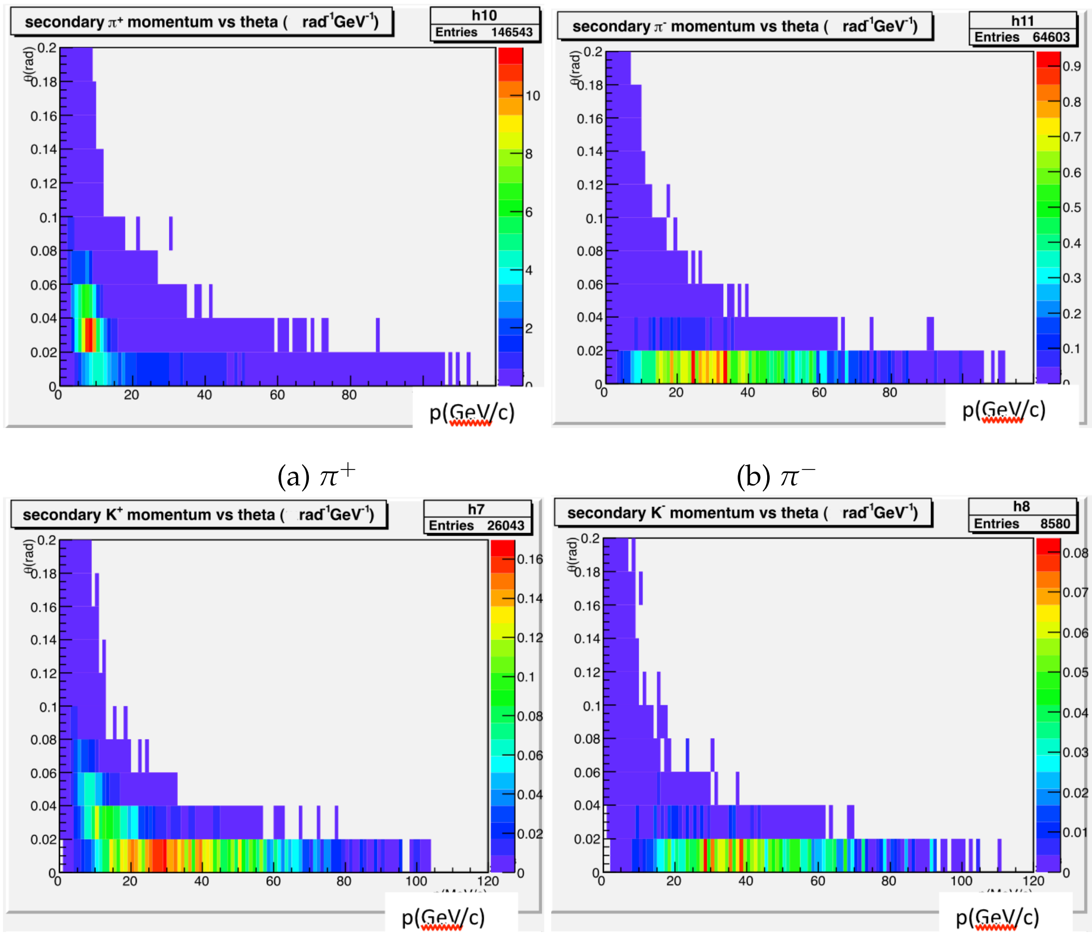

(a) π^+ (b) π^-

(c) K^+ (d) K^-

Figure 2: The four plots are in bins of momentum and polar angle for a) π^+'s, b) π^-'s, c) K^+'s, and d) K^-'s. Each bin content is proportional to the number of particles(note the different vertical scales for each plot) that gave neutrinos that interacted in the MINERνA detector for a given number of protons on target.

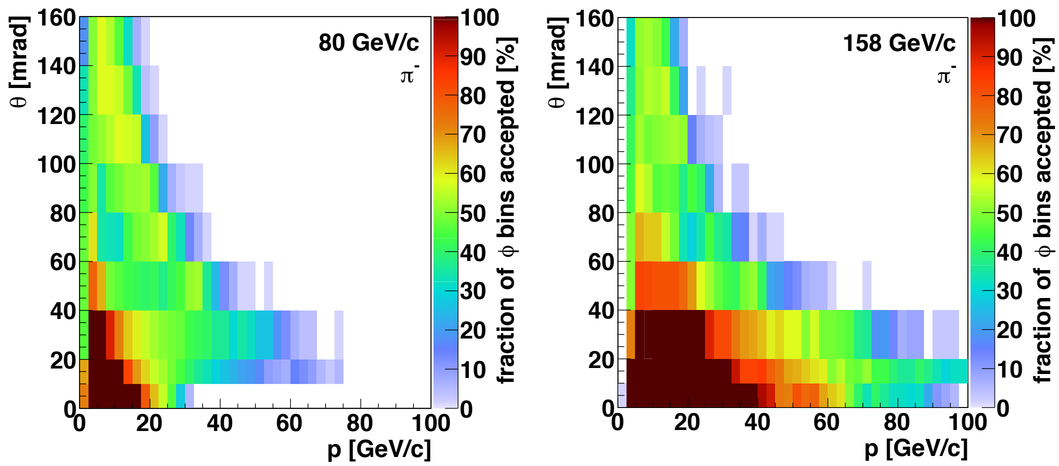

Figure 3: Reconstruction acceptance of the NA61 spectrometer for charged pions at the indicated magnetic field settings. This does not include the additional forward tracking.

3.2 MINOS+

MINOS+ [2] will be the continuation of MINOS running with the medium energy setting of the NuMI beam required by the the NOvA experiment. This will involve a reconfiguration of the current NuMI beam to achieve a higher energy broad neutrino spectrum peaking at about 9 GeV. The target and horn configuration will be different than was used in any of the MINOS settings. The new setting will be close to the MINOS medium energy setting (for which the target was moved upstream rather than the horn moved downstream), and out of the three energy settings, gave the worst agreement when the target hadron production model was tuned to reproduce the near detector event energy spectra. MINOS+ will have much higher statistics than MINOS, thus the results will be more sensitive to systematic errors in the knowledge of the simulated flux especially for sterile neutrino searches studying large Δm^2 oscillations. This is a strong motivation for improved hadron production data, that would yield a more precise neutrino flux prediction.

3.3 NOvA

The NOvA experiment [3] will be the flagship neutrino experiment at Fermilab. It will operate with two detectors of identical technologies, and will be less sensitive to uncertainties of simulations of the neutrino flux and related backgrounds since the near detector will be used to characterize the beam and its composition. However, as large statistics are accumulated in NOvA, its precision in measurements of neutrino oscillations and the scope of the near detector physics will increasingly depend on detailed understanding of the *new* medium energy beam. Thus, improved beam simulations will be necessary to fully exploit NOvA physics reach. As already noted, NOvA's competing and complementary experiment T2K has been following a similar path forward, including exposure of the T2K target using the NA61 beam and detector [4,5].

3.4 The Long Baseline Neutrino Experiment (LBNE)

The LBNE experiment [6] will be the next step in long baseline neutrino oscillation physics. LBNE's goals are to measure the mass hierarchy and CP violation in the lepton sector. The experiment will design a new high intensity beam and target that will use the 80-120 GeV beam from the Main Injector. With the measured large value of $\theta_{13} \approx 9$ degrees by Daya Bay [7], the rate of electron neutrino interactions will be high, and the corresponding effects due to CP violation and mass hierarchy become a smaller relative effect. That means the precision of the CP violation measurement will be limited by systematic errors, which provides a strong motivation for better determination of hadron production by an experiment like NA61/SHINE.

Figure 4 shows the relative hadron contributions to the total neutrino flux at the LBNE far detector site. Comparing this to Figure 3 shows that the 4.63 Tm and 9.0 Tm magnetic field settings for NA61 have good acceptance for the hadrons that contribute to the flux in LBNE.

To study the impact that NA61/SHINE can have on the LBNE flux uncertainty, the parameterization given in reference [8] was used. Predicted fluxes at the LBNE far site were

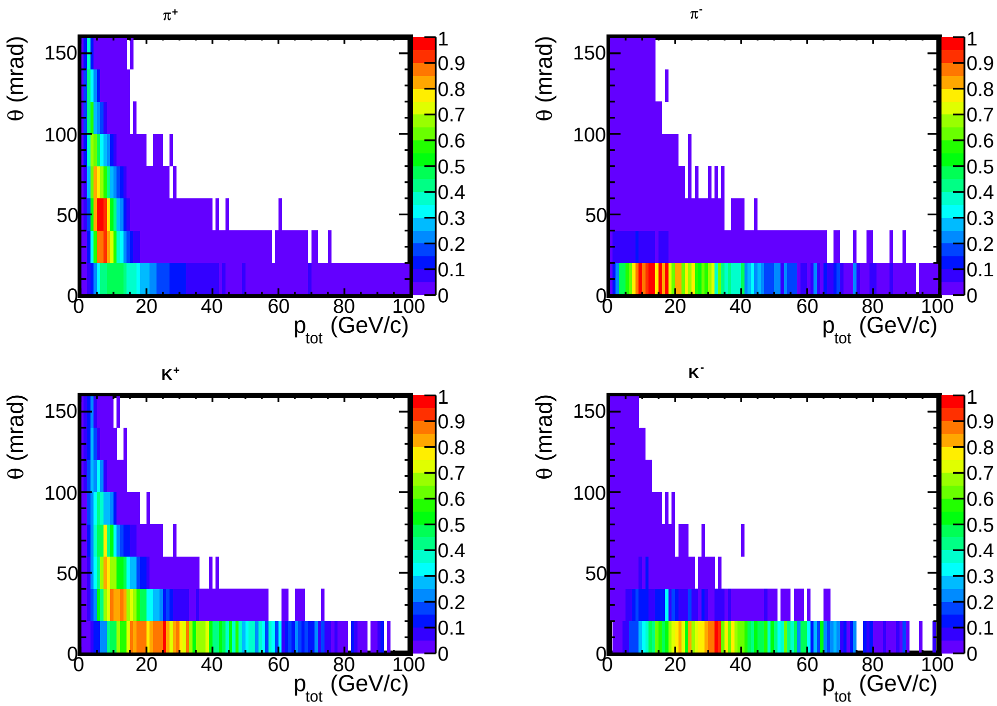

Figure 4: Pion and Kaon contributions(normalized to each hadron type) to total neutrino flux at LBNE far site.

generated for the nominal parameter values, and for 5000 sets of random throws of the parameters. For each of these parameter sets, weights for π^+, π^-, K^+, and K^- production at the target were computed, and these resulted in 5000 different predicted far detector spectra. Based on the systematic errors given in the NA61 measurements made for T2K [10, 19], NA61 could potentially make measurements at 120 GeV with 3-5% errors on the π^+ production and 10% errors on the K^+ production in the regions of phase space where there is good acceptance.

For each of the 5000 random hadron parameter variations described above, a throw is considered to be consistent with potential NA61/SHINE constraints if the hadron production weights for that throw is within the assumed errors. The resulting fractional spread of these models on the predicted far detector neutrino fluxes are shown in Figure 5. The resulting spread on the predicted ν_μ and ν_e flux at the LBNE far detector is less than 6% below 10 GeV. The expected LBNE Flux peaks around $\sim$3 GeV, with very little flux above 10 GeV.

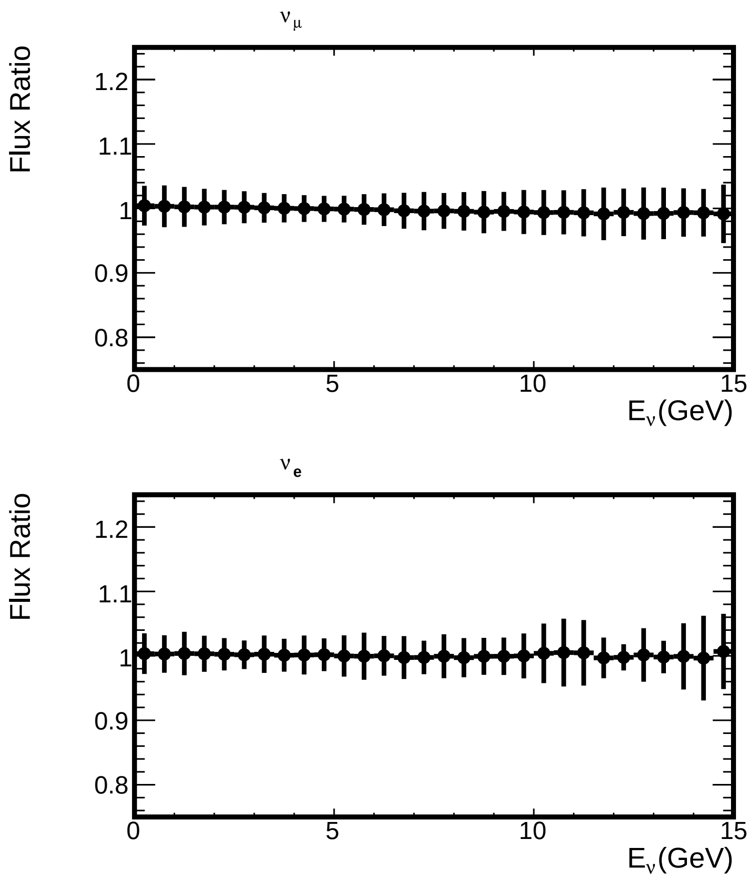

Figure 5: Predicted fractional errors on the neutrino flux at the LBNE far site using the assumed NA61 constraints, for ν_μs in the top panel, and for ν_es in the bottom panel. The forward tracking is not included here.

3.5 NuMI-X modeling

As stated earlier, determining the neutrino flux in any neutrino beam line is both essential for physics objectives and challenging. It requires detailed knowledge of hadron yields from extended targets and other complex information necessary for particle transport. The NuMI beam has, or soon will service, six experiments (MINOS, MINERvA, NOvA, MINOS+, MicroBooNE, ArgoNeut) with diverse detectors and physics programs. It is compelling that all these experiments would benefit from the development of common tools to simulate the NuMI beam line and produce a "reference flux" or a "reference beam line flux simulation". That flux and simulations can then be used to make comparisons and predictions between measurements by present and future detectors in the NuMI beam line. Tools and techniques developed for NuMI would be useful in other beam lines such as the LBNE or Booster neutrino beams.

The six NuMI experiments with seven detectors (on-axis MINOS Near Detector (ND), MINOS+ ND, MINERvA, and ArgoNeuT, off-axis (14 mrad) NOvA ND, off-off-axis (110 mrad) NOvA NDOS, and off-off-off-axis (135 mrad) (Mini)MicroBooNE) provide unique constraints for simulations. Many data sets have been collected from several target, horn, and horn current configurations. The proposed pan-experimental NuMI flux working group, for brevity called the NuMI-X Consortium, would develop simulations of a reference flux by considering and incorporating past and ongoing efforts and ideas on these matters.

Although the work to coordinate beam work among these experiments has been initiated, it is expected that the main improvement in neutrino beam simulation will have to come from precision measurements of hadronic yields, such as the measurements proposed here with NA61/SHINE.

3.6 Expected Improvement for Neutrino experiments from NA61 Data

The data collected by NA61 will enable much more accurate modeling of hadron interactions of the Fermilab neutrino beams. Currently, the estimates of overall flux uncertainties for those beams is 11-15% uncertainty [9], with the majority due to a lack of hadron production data. NA61 measurements are expected to bring that total flux uncertainty down to around 5-6% (Figure 5), a factor of 2-3 reduction in the flux uncertainty. That will in turn translate into a better understanding of neutrino detector responses, to a better understanding of absolute neutrino cross sections, and finally to smaller errors on neutrino oscillation parameters.

4 Hadron Production Data

Neutrino flux predictions require not only good knowledge of the total pion and kaon production cross-sections but additionally, and more importantly, differential cross-section information in terms of the momentum and angle (p, θ) of the produced particle or equivalently the transverse momentum and Feynman-x (p_T,x_F). These data are required for incident protons at the primary beam energy on the neutrino target's nucleus (carbon for NuMI). Data for incident protons, neutrons and pions at lower energies are also needed to constrain tertiary production.

Most of the currently available data do not cover all the phase space at NuMI or BNB. An illustration of this mismatch is shown in Figure 6.

4.1 What more is needed?

Approximately 40% of the ν_μ that interact in MINERνA and MINOS are due to pions and kaons which were not created directly by a $p + C$ collision at 120 GeV/c. Instead, these neutrinos are produced in secondary and higher order reinteraction processes like these (typical momenta of secondaries are given in parentheses) :

$$
\begin{aligned}
&p(120\,GeV/c) + C \rightarrow p(60\,GeV/c) + X \\
&\qquad\qquad \hookrightarrow p + A \rightarrow \pi^+(20\,GeV/c) + X \\
&\qquad\qquad\qquad\qquad \hookrightarrow \pi^+ \rightarrow \mu^+\nu_\mu(8\,GeV/c)
\end{aligned}
$$

$$
\begin{aligned}
&p(120\,GeV/c) + C \rightarrow \pi(30\,GeV/c) + X \\
&\qquad\qquad \hookrightarrow \pi + A \rightarrow \pi^+(15\,GeV/c) + X \\
&\qquad\qquad\qquad\qquad \hookrightarrow \pi^+ \rightarrow \mu^+\nu_\mu(7\,GeV/c)
\end{aligned}
$$

Reinteractions occur copiously in the few interaction length targets used in neutrino beams. Figure 7 shows the fraction of pions from target reinteractions as a function of the primary beam momentum. One can see that, as the beam momentum increases, the fraction of pions from reinteractions grows. The fraction also grows as the pion momentum decreases.

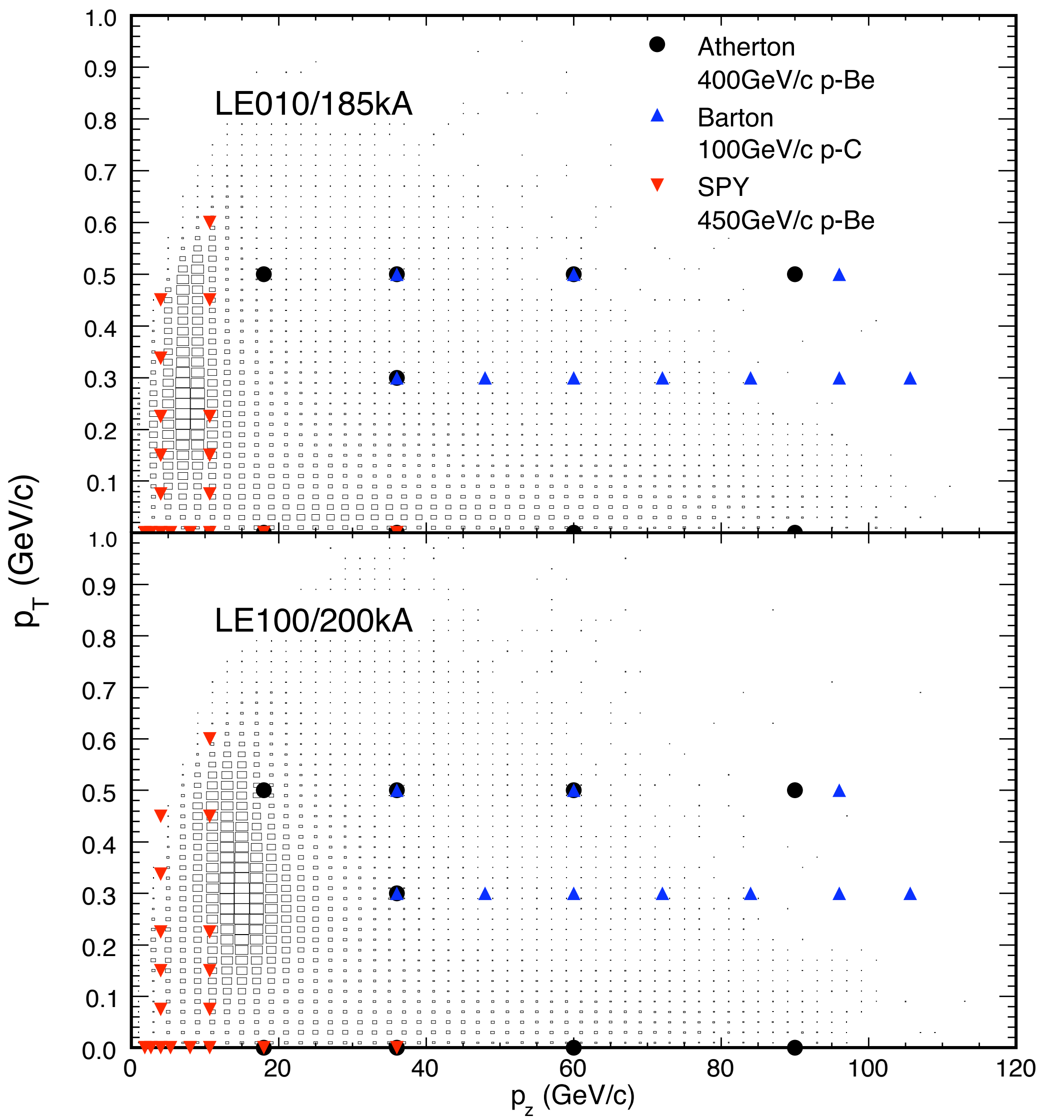

Figure 6: The distribution of transverse and longitudinal momentum of π^+ that contribute to neutrinos at the MINOS Near Detector for two different beam configurations, low energy (LE010/185kA) and medium energy (LE100/200kA). The size of the box is proportional to the number of charged current neutrino events in the MINOS Near Detector that come from π^+ momentum $p = (p_z, p_T)$. Overlaid are the points that indicate the part of the phase-space measured by the three relevant hadron production experiments (taken at higher primary energies) [13–15]. It should be emphasized that the measurements shown are not taken with a 120 GeV proton beam, they are scaled from other energies, and have an error associated with the particular scaling model employed.

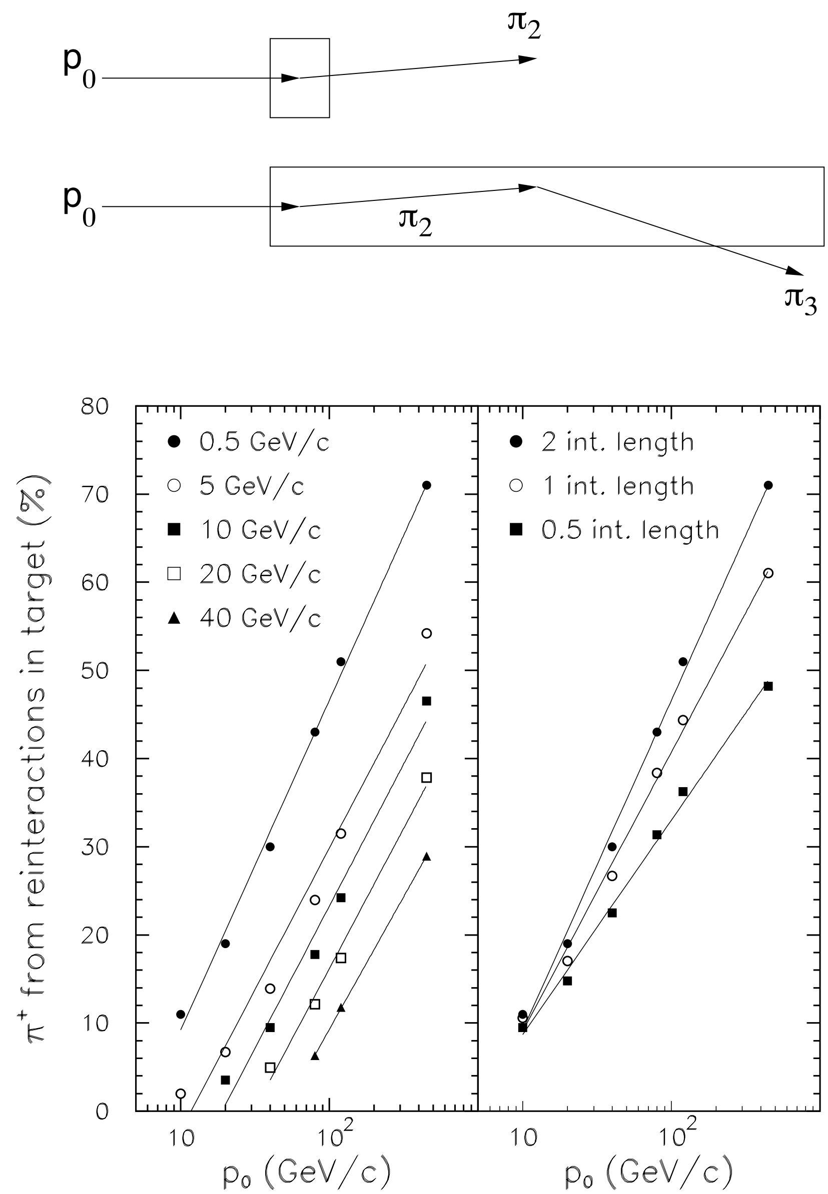

Figure 7: Pions created in primary proton interactions can escape out of the thin target without re-interaction. For a long target there is a high probability that a pion will re-interact (top). The calculation of the fraction of tertiary π^+ production from re-interactions in a graphite target as a function or primary beam momentum p_0 is shown. The calculation was done using FLUKA [18]. The left plot shows the re-interaction fraction for a two interaction lengths long target with several secondary pion momentum thresholds (p_z). The right plot shows the re-interaction fraction for three different lengths of the target.

proton+pion event totals	**Incident proton/pion beam momentum**		
Target	120 GeV/c	60 GeV/c	30 GeV/c
NuMI (spare) replica	(*future*)		
LBNE replica	(*future*)		
thin graphite ($< 0.05\lambda_I$)	(*future*)	3M	(T2K data)
thin aluminum ($< 0.05\lambda_I$)		3M	3M
thin iron ($< 0.05\lambda_I$)	(*future*)	(*future*)	(*future*)
thin beryllium ($< 0.05\lambda_I$)	(*future*)	3M	3M

Table 3: A table of proton+pion event totals for target and beam settings which are relevant to US long baseline neutrino experiments, that would be run after the CERN 2013-14 shutdown. Proton and pion data may be taken simultaneously with the proper trigger settings. The first set of runs, requested in 2015, are labeled with 3M (the number of incident pion and proton triggers), and the other relevant runs would take place in the *future*, possibly during 2016. For the 2015 runs we wish to start with the lower energy ones first where the FTPC measurements are less important.

Approximately 20−40% of the pions which yield neutrinos in the peak of the NuMI low energy beam ($p_\pi \approx 5 - 10\,\mathrm{GeV/c}$) were created from tertiary hadrons produced by secondary interactions in the target. A good understanding of reinteractions, both in the target and in other beamline elements such as the focusing horns, decay pipe gas and walls, and target hall air, is important for precision flux and oscillation experiments. A comprehensive program would combine thick (replica) target data at the primary beam momentum with thin target data for incident π, K and p taken at 120 GeV/c and one or more lower momenta in the range 20−30 GeV/c to span the kinematic range interesting for NuMI and LBNE. Thin carbon and Be data are the most important, but data on Al and Fe would also be useful as shown in Table 3.

5 Proposal for NA61/SHINE Measurements

As described in Section 4 we wish to collect a series of data sets that will fill in the gap of existing hadroproduction data pertinent to neutrino flux predictions for US facilities. The following section describes in some detail the analysis steps required to convert the collected data into a form needed for the neutrino flux machinery. Where applicable specific US contributions and personnel are described. Presently the cycle time between data taking and publication is 4-5 years. The US groups wish to contribute in ways that will speed up this process.

5.1 Physics Goals and Measurement Technique

The primary goal of the proposed program will be to measure the inclusive, double differential cross-section for charged secondaries (πs, Ks, and protons) as a function of secondary momentum and angle. Thus given a target thickness (t) and number density (n), interaction length (λ), interaction cross-section (σ), the probability that an incident proton interacts is given by:

$$P(t) = 1 - e^{-t/\lambda} = 1 - e^{-n\sigma t} \approx n\sigma t \text{ (thin target)} = \frac{\rho N_A t}{MW}\sigma \tag{1}$$

where ρ is the density, N_A Avagadro's number, and MW the molecular weight (12 for carbon). In a differential form this becomes:

$$\frac{d^2P_\alpha(p,\theta)}{dp\,d\theta} = nt\frac{d^2\sigma_\alpha(p,\theta)}{dp\,d\theta} = \frac{1}{N_{prot}^{inc}}\frac{d^2N_\alpha(p,\theta)}{dp\,d\theta}\ ,\alpha = \pi, K, \text{ or } p \tag{2}$$

where N_{prot}^{inc} is the number of incident protons on target. The true number of events must be unfolded from the observed data by taking into account backgrounds (B) and detector response:

$$\frac{d^2N_a^{meas}(p_r,\theta_r)}{dp_r\,d\theta_r} - \frac{d^2N_{back}(p_r,\theta_r)}{dp_r\,d\theta_r} = ntN_{prot}^{inc}\sum_\beta\int\int dp_t d\theta_t \frac{d^2\sigma_\beta(p_t,\theta_t)}{dp_t d\theta_t}R_{a\beta}^{det}(p_r,\theta_r;p_t,\theta_t) \tag{3}$$

where N_{back} is the target-out background, a refers to the particle identification (PID) selection category (π-like, K-like, or p-like), β refers to the true particle type (π, K, p, etc.), $R_{a\beta}(p_r,\theta_r;p_t,\theta_t)$ contains the detector response effects (efficiency, acceptance, resolution, and migration) plus any multi-particle efficiency corrections, and the subscripts t and r refer to "true" and "reconstructed" respectively.

The target-out background can be measured with sufficient precision by taking about 5% of triggers with the target removed. The number of incident protons is given by the incident beam selection, n and t are determined by the target employed. The more challenging $R_{\alpha\beta}(p_r, \theta_r; p_t, \theta_t)$ can be constructed partially from data, where individual detector responses can be extracted accurately, and partially from simulations, which can be used, for example, to accurately calculate the complex acceptances of decaying, charged particles in a magnetic field. Such an approach succeeded in the analysis of the HARP data for the MiniBooNE experiment, and in the analysis of NA49 and NA61 data for T2K. The goal is to measure $d^2\sigma_\alpha/dpd\theta$ with a total error (systematic(dominate) + statistical) of 3-5%.

5.2 Beam Characteristics

The NA61/SHINE experiment resides on the CERN North Area's H2 beam line, a secondary beam from the H2 target. The H2 beam has delivered hadron beams in the energy range 13 GeV/c to 350 GeV/c, and lead and beryllium ion beams in the range 13A GeV/c to 158A GeV/c. It is expected that argon and xenon beams will become available in the future. Figure 8 shows one of the configurations used to select ion beams.

This proposal seeks to use hadron beams from 120 GeV/c down to a lower limit of 30 GeV/c of pions and protons. The momentum spread in the beam is typically lower than 1% with an RMS width of slightly larger than 2 mm at the lowest momenta and 1.2 mm at 158 GeV/c.

The beam line is equipped with a special differential Cherenkov counter, the Cherenkov Differential Counter with Achromatic Ring Focus (CEDAR). The counter is able to cleanly select a hadron type by adjusting the pressure of a gas radiator and tuning the angular focus of the counter to the appropriate momentum for that particle type (protons, pions, or kaons). The efficiency for typical settings is roughly 95% with a contamination of less than 0.8%.

Figure 9 shows two pressure scans with the CEDAR counter which measure the relative fractions of protons, pions, and kaons present in the beam. The left panel shows a scan at 31

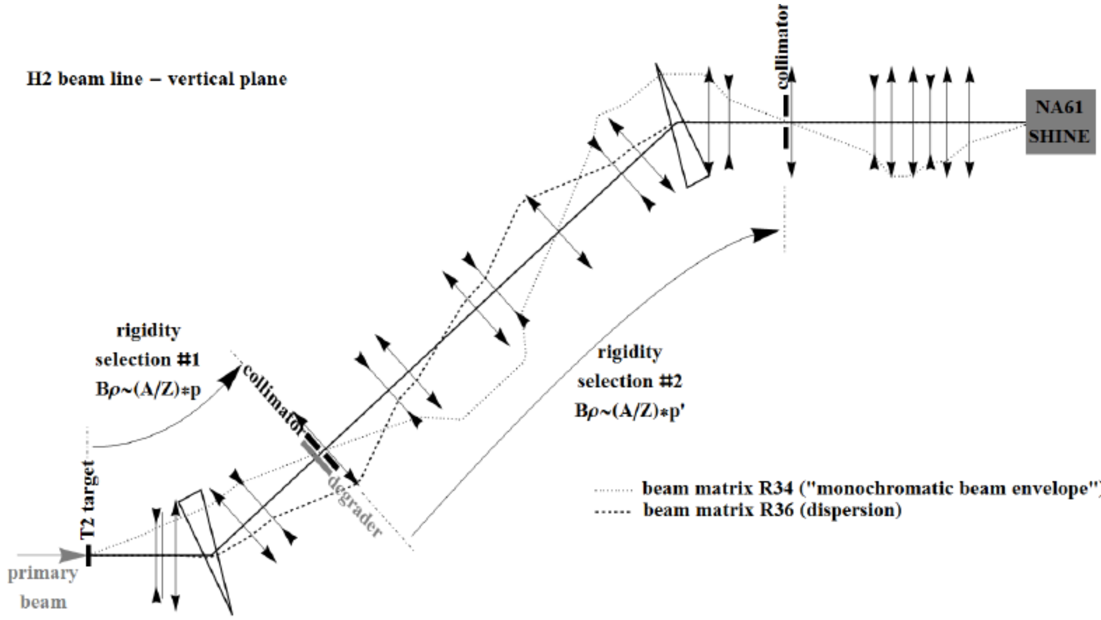

Figure 8: The optics for the H2 beam line for ion running that shows the two momentum selection sections and the degrader. (from reference [12])

GeV/c, where the $\pi : K : p$ fractions are 84% : 1.7% : 14%, and the right panel shows a scan at 158 GeV/c, where the $\pi : K : p$ fractions are 37% : 3% : 60%. At 120 GeV/c the $\pi : K : p$ fractions are approximately 48% : 2% : 50%.

5.3 Trigger Setup

The H2 hadron beamline yields a secondary beam that consists of electrons, pions, kaons and protons. At momenta above approximately 120 GeV/c the beam is dominated by protons, while below 120 GeV/c the beam is dominated by pions, and at very low energies electrons. There is a small component of kaons present also, at the level of a few percent. For our purposes, we wish to trigger primarily on both pions and protons, and employ the CEDAR counter to discriminate between the two.

The programmable trigger module is normally set up for four types of triggers. Each of the triggers may be prescaled to only trigger every Nth occurrence of the trigger, where N is greater than zero. A typical trigger scenario has T1 trigger signifying the presence of a

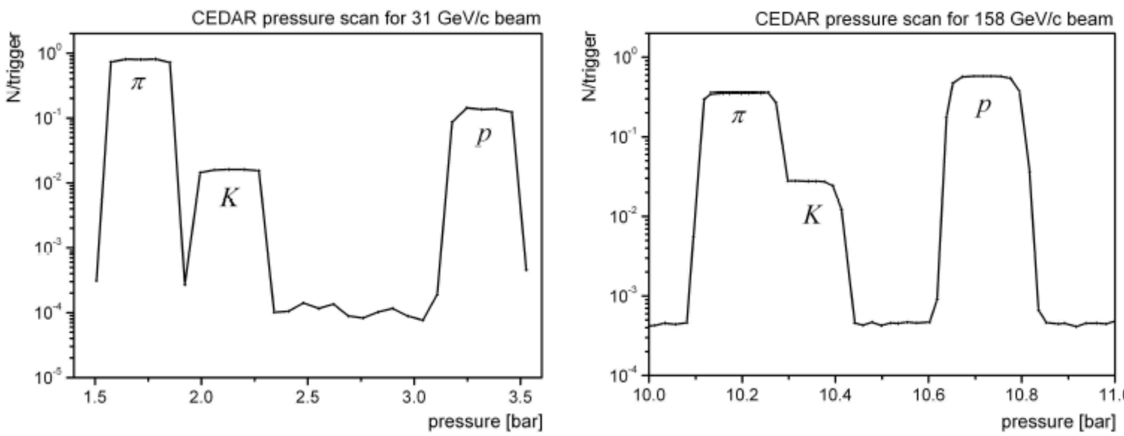

Figure 9: Two pressure scans for the CEDAR particle identification in the H2 beam line. The left panel is for a 31 GeV/c momentum setting and the right panel is for a 158 GeV/c setting. (from reference [12])

desired beam particle (normally a proton or a pion identified by the CEDAR), T2 will signify that a desired beam particle interacted in the target. In normal operating mode, T2 is not prescaled, while T1 is recorded with a prescale factor of $\sim$ 250. The T3 and T4 triggers are normally set like T1 and T2, respectively, however no CEDAR identification of the beam particle is required. Both are prescaled and the data provide an unbiased sample of CEDAR data.

In addition to normal beam running, roughly 5-10% of the data is taken with the target removed from the beam. That target-out data allows a crucial subtraction of no-target related interactions of protons along the beam's path into and through the detector. For example, the number of subtracted target-out events [16] for the 158 GeV/c proton-carbon analysis, after interaction vertex cuts, was 11k, subtracted from 377k target-in events.

5.4 Event Rates

The NA61/SHINE data acquisition was able to record $750,000$ to $1,000,000$ events per day, which includes 10% target-out data, with a beam setting of 120 GeV/c during our pilot run in 2012. At lower energies the fraction of protons or pions in the beam will change that rate. We anticipate $\sim$ 3-5 days will be needed per setting, where roughly an equal number of pion and proton interactions are recorded.

5.5 Computing Plan

We intend to use the CERN/NA61/SHINE computer and data storage resources to analyze the data. In the first run (five settings) we expect to record a total of 15M events corresponding to disk space of $\sim$ 50 TB, a modest amount of data relative to the total NA61/SHINE data store. The computing power required for analysis of the data is also not large by NA61/SHINE standards since the proton-carbon interactions have lower multiplicity than A-A collisions, and hence can be accommodated by the CERN/NA61/SHINE infrastructure. Our experience suggests that it will take 1-2 years of data processing and calibration effort to bring a data run to a state where it is ready for physics analysis, and then another year before publication. Since the work is done in parallel, we estimate that all runs will have published results within 2-3 years of taking the data. There is a vigorous effort directed at making the calibration process more streamlined, which could allow publications on a shorter time scale.

5.6 Data Processing

There is chain of calibrations that must be performed on the data prior to final data analysis. These steps include calibrations of the detector position offsets, drift velocities, timing offsets, and energy loss (which is critical to the particle identification), and many of these will be briefly described below. Members of the USNA61 group are currently responsible for some of these tasks.

5.6.1 Beam Line and Gap TPC Calibration

The three beam position detectors (BPDs) are located upstream of the NA61/SHINE TPCs and are used to ensure that the beam particles strike the target. Initially these are aligned using surveyor measurements. Additional corrections to the alignment of the three detectors with respect to each other are obtained by comparing the residual position offsets for each BPD between the recorded clusters and the fitted tracks. The relative alignment of the BPDs to the TPCs is done by examining the impact parameter between the primary TPC tracks and the BPD tracks, especially for runs with low magnetic field settings.

The Gap TPC (Time Projection Chamber) is normally calibrated using reconstructed tracks from the other TPCs, and therefore requires calibrating them first. A procedure was developed by USNA61 members to calibrate the Gap TPC relative to the BPDs (Beam Position Detectors), using beam tracks. This allows the calibration of all TPCs to be done in parallel. This produces a correction factor to the drift velocity. Since the June 2012 USNA61 pilot run had no magnetic field, and the July 2012 run had only one magnet turned on, this technique will be used to generate Gap TPC drift velocity corrections for both USNA61 pilot runs.

5.6.2 Drift Velocity Calibration

The drift velocity is a function of pressure, temperature and the high voltage. Those values are logged in a database and are used to smooth out rapid fluctuations and correct the drift velocity to a normalized value. Additional long-term corrections are done by looking at the vertical position of clusters that are the farthest from the readout plane (i.e. the maximum drift length). This distance is fixed by the TPC geometry and should be constant over time. Any deviations from this value indicate a change of the drift velocity, and this is used to determine corrections to the drift velocity in the TPCs as a function of time. The absolute calibration of the drift velocity is done by comparing the vertical position of clusters in the main TPCs and comparing that to the position of hits recorded in the time-of-flight system.

5.6.3 Residual Corrections

After the detector geometry and drift velocity calibrations, there are still small local distortions that remain. By comparing the residual differences between the locations of clusters of TPC hits to the locations of reconstructed tracks, any remaining necessary corrections can be determined. Members of the USNA61 group are currently responsible for generating these corrections and assessing their quality.

5.6.4 $E \times B$ Drift Corrections

The TPCs use a magnetic field that is oriented parallel to the drift electric field. If perfectly parallel, the drifting electrons would move perpendicular to the pad rows, along the E field, without feeling any effect of the B field (since the drift velocity would be parallel to the B field). In actuality the E field and B field are not parallel due to field inhomogeneities. This results in the electrons not drifting in a straight line to the pad rows but in curved paths. The present inhomogeneities in the magnetic field will generate a deviation of up to 5 cm for the arrival point of the electron clusters to the readout pads and must be corrected. Two corrections applied are generated via simulation. The space point correction routine generates 3D drift velocity tables using a 3 cm grid width and measured field maps. Points in between are linearly interpolated. In the simulation the integration starts at the defined space point and ends at the pad plane. The second geometrical correction is a result of the track curvature in the pad plane. The effect depends on the track angle relative to the pad direction and shifts the center of the charge cluster used in track reconstruction. These corrections must determined for different run periods specifically after changes to the magnetic field strengths.

5.6.5 dE/dx Calibration

The precise measurement of energy loss and its use for particle identification is a primary design goal of the NA61/SHINE tracking system. The expected momentum distribution of reconstructed tracks for the US program will range from several hundred MeV/c up to about 120 GeV/c. The measurement spans the full range of the energy loss function. Therefore the dE/dx calibration is important to the US program.

A simultaneous calibration of the electronics and gas gain is performed by releasing electrons with a known energy spectrum into the TPC drift volume. Radioactive ^{83}Kr is used for this purpose. ^{83}Kr, with a half life of 1.9 hours and excitation energy of 41.6 keV, is created from a ^{83}Rb source housed in a volume by-pass of the TPC gas recirculation system and injected into the TPC gas. Calibration data are taken at maximum data acquisition rate. For a source intensity of 180 MBq, about 1000 Kr decays are recorded in a single readout cycle. In a data taking period of about 2 hours, this permits the production of high statistic charge spectra for all read-out pads yielding a precision of better than 1.0% for the energy loss in the TPC. These *Kr* calibration runs are typically taken before and after each SPS running period of 6-8 weeks. US graduate student Ben Messerly (University of Pittsburgh) is presently being trained as a TPC gas system and calibration run expert. New University of Pittsburgh postdoc Nick Graf will start taking responsibility for the dE/dx calibration.

5.6.6 Time-of-Flight Calibration

The TOF-L and TOF-R counter arrays (left and right) are useful in cross-checking the dE/dx particle identification up to momenta of around 5 GeV/c. Therefore a calibration of that system is necessary for a complete understanding of the particle identification. The TOF calibration (time offset, slew correction, etc.) is obtained by equalizing and optimizing the TOF response with particles already well-identified by the TPC dE/dx technique. The technique can be iterated to obtain a self-consistent set of calibration constants.

5.7 Data Analysis

The procedures used for data analysis and cross section measurements include event and track quality selection plus most importantly for the US program, the identification and separation of pions, kaon, protons and neutrons. The following section will describe in some detail each of these steps.

5.7.1 Event Selection

A described earlier a secondary hadron beam is produced from 400 GeV/c protons extracted from the SPS in slow extraction mode. The beam is transported along the H2 beamline toward the experiment. Particles from the secondary hadron beam are identified by two Cherenkov counters, a CEDAR and a threshold counter, known as C1 and C2, respectively and can be used in the trigger to select incoming particle type, usually a proton or pion. A selection based on signals from these Cherenkov counters allows the identification of beam protons with a purity of about 99%.

A schematic of the trigger counter layout is shown in Figure 1. Two scintillation counters S1 and S2 located before the target in conjunction with two veto counters V0 and V1, containing a 1-cm-diameter hole, provide the incoming beam definition on the target. The S1 counter provides also the timing (start time for all counters). Good beam particles are therefore selected by the coincidence $S1{\cdot}S2{\cdot}\overline{V0}{\cdot}\overline{V1}{\cdot}C1{\cdot}\overline{C2}$. The trajectory of individual beam particles can be measured in a telescope of beam position detectors along the beam line (BPD-1, -2 and -3). This is important for the US program since we can therefore weight the incoming beam profile to match the profile that will impinge onto proposed neutrino production targets.

Interactions in the target are selected by an anti-coincidence of the incoming beam protons with a small, 2-cm-diameter, scintillation counter (S4) placed on the beam trajectory, after the target, between the two vertex magnets. This minimum bias trigger is based on the disappearance of the incident proton. Interaction events are selected by $S1{\cdot}S2{\cdot}\overline{V0}{\cdot}\overline{V1}{\cdot}C1{\cdot}\overline{C2}{\cdot}\overline{S4}$ and BPD signals consistent with one incoming particle. This criterion removes contamination by interactions upstream of the target and typically reduces the number of triggered events to selected events by $\sim$ 20%.

5.7.2 Track Selection

Track selection is typically very similar across different reactions and beam momenta, but the cut values are usually tuned for each individual analysis. Cuts that are typical for neutrino data measurements will be discussed here.

In the SHINE analysis framework, there is a distinction between tracks and vertex tracks. Tracks are fit to clusters of hits. Vertex tracks are fit to the same clusters with the additional constraint of being fit to a common vertex. Typically vertex tracks are used in analyses, and they are required to have a good fit in the reconstruction. Related to this, there is usually a cut on the impact parameter (distance between the vertex position and the track at the same z value).

At this point, analyses usually consider different track topologies. The topologies are grouped in two different ways. Tracks with different momenta and angles will travel through different TPCs, so tracks are grouped by which TPCs they make hits in. The different topologies may have different selection efficiencies, and after an efficiency correction are combined to yield an overall multiplicity for a given bin in (p, θ) phase space.

Further cuts are made on the number of reconstructed clusters there were in each TPC. Another cut is the "z_{last}" cut. The last reconstructed cluster of a track must have a z position greater than a decided value. We must include a "θ/ϕ" cut to remove tracks that exit through the top and bottom faces of the TPCs. Because the differential cross section is symmetric around ϕ, we can cut on ϕ without worrying about biasing our results. For analyses which use the ToF detectors, the last cut is usually to require a hit in one of the ToF detectors.

5.7.3 Particle Identification and Fitting

Depending on the particle species being studied, a vertex or a dEdX/ToF analysis is used. Neutral particles that do not decay too quickly or too slowly (particles that decay inside the detector volume), can be studied with a vertex analysis. These can include K_0 and Λ_0. Charged particles can be studied with a dEdX/ToF analysis. These particles can include p, $\bar{p}$, K^+, K^-, π^+,π^- and d, but this depends on the amount of data taken and the reaction being studied. Figure 10 and Figure 11 show an examples of how the TPC and TOF-L/R systems can be combined to provide particle separation between Ks, πs, and protons.

Above approximately 10 GeV the variance of the m^2 data in the ToF is too large to separate particle species. At higher energies particle ID will rely on the dEdx energy loss. Figure 12 shows the dEdx energy loss as a function of momentum for particles from p+p interactions at 80 GeV.

5.7.4 Final Cross Section Extraction and Expected Error

Cross-section extraction will follow the general analysis outline described in Ref. [19] and used earlier in Ref. [20]. Tracks with the appropriate particle identification will be binned in p and θ.

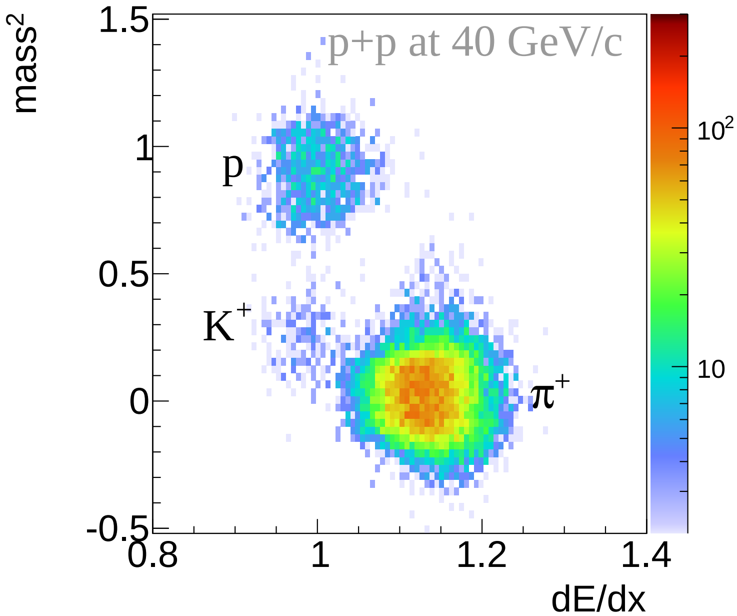

Figure 10: m^2(GeV^2/c^4) versus the TPC dE/dx(MIP) from the TOF-L/R system for positive particles within the momentum range 2-4 GeV/c.

Background-only runs are taken with the target removed, and the same reconstruction and cuts applied in order to correct for out-of-target interactions. In Ref. [19], the interaction probabilities with the "5% interaction length" carbon target in and out were $(6.022 \pm 0.034)\%$ and $(0.709 \pm 0.007)\%$ respectively.

Normalization is performed using data from a minimum bias trigger to calculate the interaction probability. The target-out result is subtracted to yield the interaction cross-section.

Figure 13 shows the expected statistical error for one million good-quality triggers in NA61. The statistical error is shown for each bin of momentum and angle. Over the range of interest of the Fermilab long-baseline program (see Figures 2 and 4), the statistical errors are below 3% in each bin.

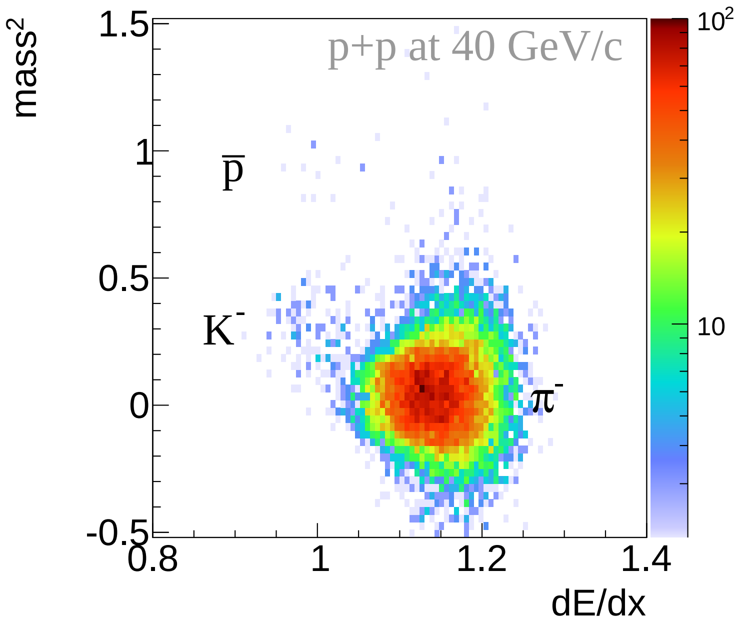

Figure 11: m^2(GeV^2/c^4) versus the TPC dE/dx(MIP) from the TOF-L/R system for negative particles within the momentum range 2-4 GeV/c.

5.7.5 Expected FTE Required for Data Analysis Completion

As listed in Table 3 US-NA61, in the near term, wishes to collect a series of thin target (Carbon, Aluminum, and Beryllium) data runs using both proton and pion beams at 120 and 60 GeV/c. To ensure a reasonable time between collection and production of publishable data ($\sim$ 2.5 years) we estimate the required number of FTE under the following assumptions. The analysis of the runs will be grouped such that the detector will be in a similar magnet and beam configuration so to have common detector calibrations. A proposed run grouping for data analysis is:

1. 120 GeV/c: $p + \text{C}$ and $p + Be$
2. 120 GeV/c: $\pi + \text{C}$ and $\pi + Be$

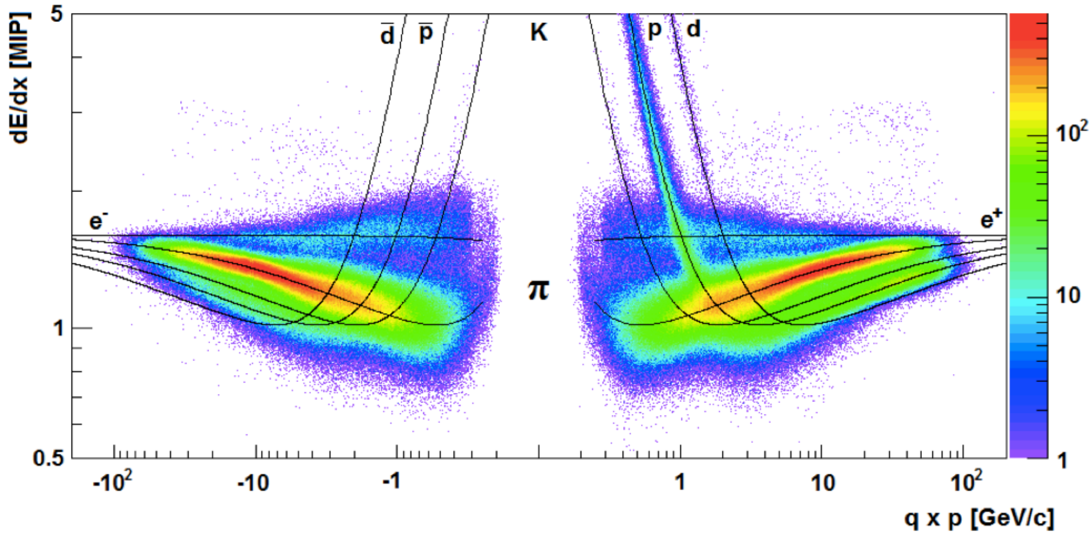

Figure 12: Energy loss in the TPCs for positively (right) and negatively (left) charged particles as a function of momentum measured for p+p interactions at 80 GeV/c. Reproduced from [12].

3. 60 GeV/c: $p + C$, $p + Al$, and $p + Be$
4. 60 GeV/c: $\pi + C$, $\pi + Al$, and $\pi + Be$

We estimate that a single postdoc would be responsible overall for each energy setting (a total of 2 postdocs), included all beam particle type and target material configurations for that energy setting. A single graduate student would be responsible for the analysis of a specific beam particle type and energy but also all target material configurations using that beam. This work would therefore require a total of 4 graduate students and 2 postdocs to complete the analyses of the initial US-NA61 data runs. As can be seen in Table 1 this estimate is well matched to the expected manpower commitments anticipated from the participating US institutions.

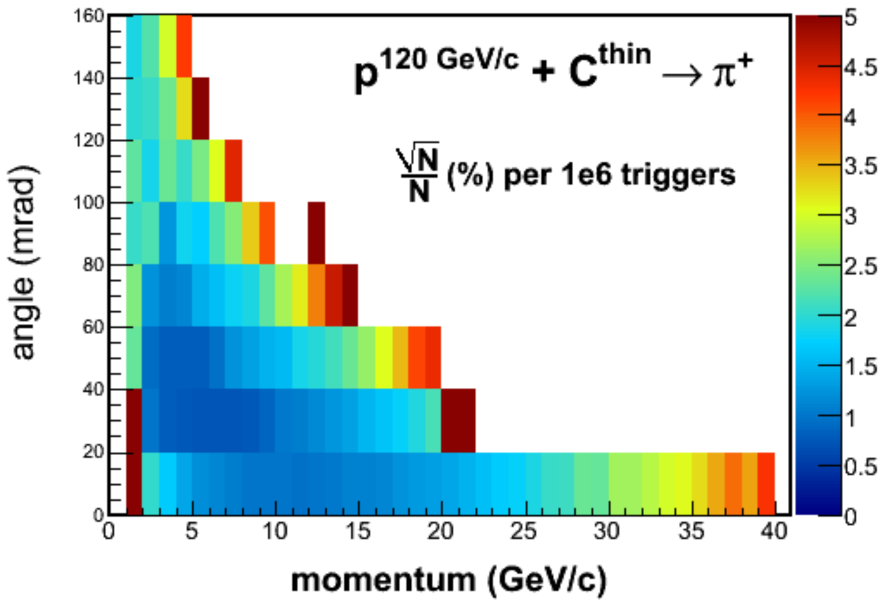

Figure 13: A representation of the expected statistical errors for bins in momentum and angle for produced pions in one million proton events in NA61. Over the range of interest for the Fermilab long-baseline program the statistical error is less than 3% (see Figure 4). The calculation includes production statistics and detector acceptance, but not data quality selection cuts.

6 US NA61/SHINE Detector Upgrade Contributions

6.1 Electronics Upgrade

A proposed US hardware contribution to NA61/SHINE is participation in the upgrade of the readout electronics. The present ToF system is based on FASTBUS/CAMAC and therefore NA61/SHINE is having a difficult time finding spare parts or expanding the number of channels that are read out. NA61/SHINE therefore wishes to replace it with a more modern system. The 4200 (including 15% spares) channels that will be replaced are dominated by the ToF but other detectors will also be included in the upgrade. The preferred schedule driver for the new electronics is the start of the 2015 SPS run period.

The chosen electronics option is readout boards based on the DRS chip developed at PSI, Switzerland [21]. The major design criterion for the system is a timing resolution of less than or equal to 60 ps specified by the ToF. As described in the electronics section of the status report in detail, precision timing is achieved by waveform sampling at 5 GSPS rates (*i.e.* 200 ps between sampling bins). The DRS ASIC is a waveform digitizer employing switched capacitor arrays. The detector signals are sampled and their charges stored in capacitors arrays at a gigahertz rate. The stored charges are then read out and digitized at a much lower rate (MHz) using commercial analog-to-digital converters (ADC). The availability of a digitized waveform eliminates the need for separate TDC and ADC channels.

The design being developed by the University of Geneva (lead by Alessandro Bravar) is based on the DRS ASIC mounted on a 6U format 32 channel input board using a VME crate/backplane for the mechanics, power distribution, and control signals. The design and layout of the 6U motherboard, power distribution will be supported by the electronics shop at the University of Pittsburgh which designed the ATLAS L1 Receiver system [22]: a system of similar size and complexity. The Pittsburgh group will be responsible for the procurement, assembly, testing and delivery of the 6U motherboards. It is estimated that the total cost of the delivered and tested 6U boards ($\sim$130 in total) is 115k$ (+ 30%). The design and layout of the 6U motherboard (electronics shop labor costs) will be covered by the University of Pittsburgh. The cost of the 9U motherboards including control components and full assembly will be supplied by the DOE/University of Pittsburgh.

All electronics production will be outsourced. The expected lead-time (submission of PO and delivery) of the DRS ASICS from PSI is six weeks. All other commercial electronics components should have similar or shorter lead-times. It is optimal for the electronics to be ready for the latter part of the 2015 SPS run and therefore the schedule, as presented earlier, is quite aggressive. However the precise 2015 delivery time is not critical as the old electronics will be left in place while the new electronics are being installed allowing the signal inputs to be switched between the two systems for commissioning and debugging.

6.2 Forward Tracking Upgrade

The forward tracking subproject is intended to allow the measurement of secondary protons in the moderate- to high-x region. Our calculations show that these protons are responsible for up to 25% of the ν_μ flux in the NuMI beam and likely a comparable fraction in the LBNE beam. A secondary goal of the system is to measure the high-momentum part of the π^+ production.

The NA61 detector is designed primarily to track particles that bend out of the beam; only one small tracking detector, the "Gap TPC" (GTPC), covers the forward region. We propose to instrument the forward region with two TPCs, one immediately upstream and one immediately downstream of the MTPCs. The new TPCs will have electric field and readout geometry based largely on the existing NA61 TPCs, and will use existing spare electronics.

6.2.1 Physics requirements and geometrical constraints

The new TPCs must cover the gap between the MTPC fiducial areas with several centimeters of overlap for cross-calibration. They must also be constructed with minimal material that could shadow the MTPCs. Ideally, the chambers should have enough extent in the longitudinal direction to separate protons from π^+ at momenta below ~ 75 GeV/c. The upstream chamber will also sit in a relatively confined space approximately 78 cm wide in the longitudinal direction, with obstructing cable trays about 10 cm above the elevation of the MTPC field cage.

A final consideration is that, for heavy-ion physics, the chambers should be capable of reconstructing many-particle events. This, along with the availability of existing electronics, was the motivation for using TPCs instead of a series of drift chambers.

Higher-rate running conditions are expected to generate enough tracks in the beam region so that out-of-time tracks may produce significant backgrounds. Out-of-time tracks are reconstructed as spatially separated tracks. In order to reject these tracks, successive field cages will have opposite drift directions so out-of-time tracks will appear unconnected at chamber boundaries. This "tandem TPC" concept originated with the NA61/SHINE Budapest group and will be implemented for the first time here.

6.2.2 Impact of Forward Tracking on LBNE

Figure 14 shows the predicted acceptance in phase space for the proposed forward tracking upgrades. Comparing this to Figure 3, we can see that it fills in the low angle region as expected. Figure 15 shows the predicted ν_μ flux at the LBNE far detector. Also shown on it by the dotted line is the flux that results from secondary particles ($\pi^{\pm}$, $K^{\pm}$, p and n) that are in the region of phase space currently covered by NA61. The dashed line shows the improvement with the additional acceptance with the proposed forward tracking.

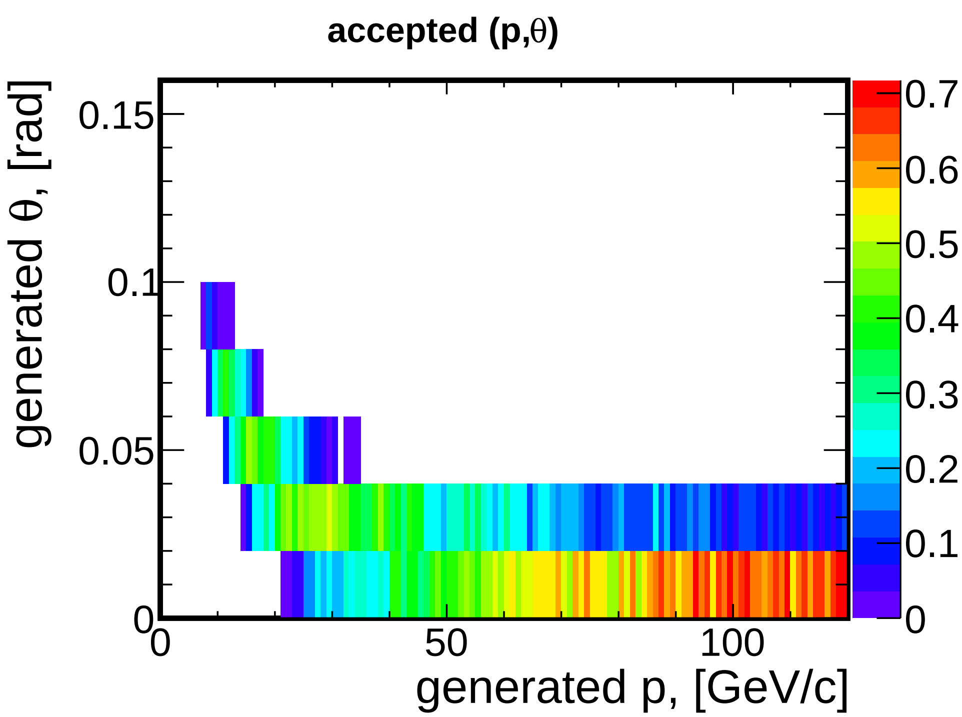

Figure 14: The predicted acceptance of the proposed additional forward tracking with the 4.63 Tm magnetic field. Here tracks are required to also go through the gap TPC.

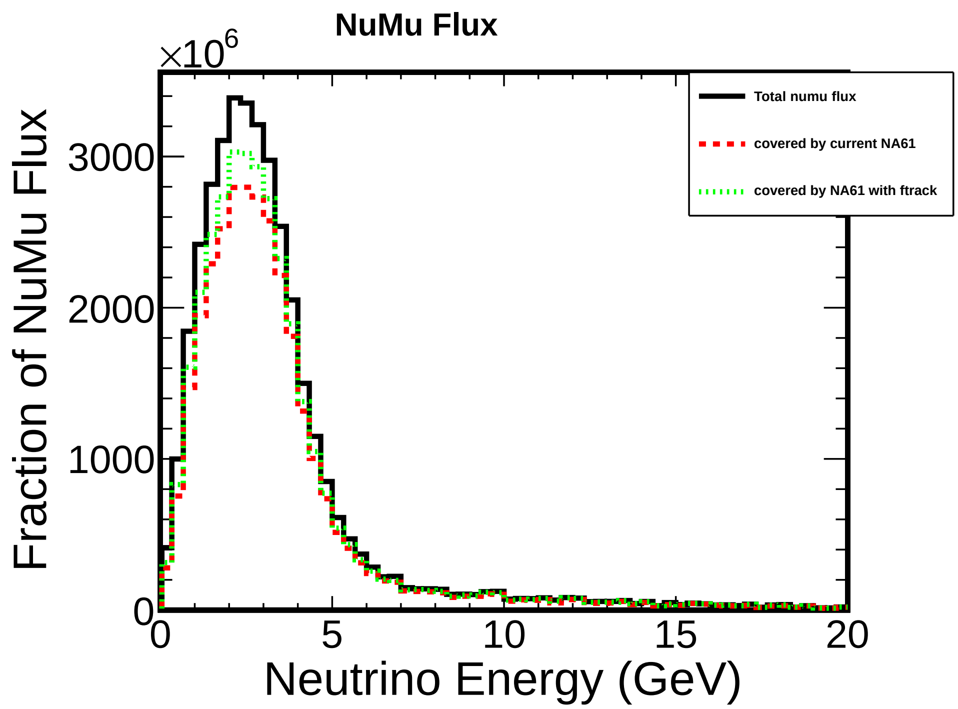

Figure 15: The predicted far ν_μ flux at the LBNE far detector. The dotted green line shows the flux resulting from secondary $\pi^{\pm}$, $K^{\pm}$, p and n that are within the acceptance of the current NA61 detector. The dashed line shows also includes particles in the region of acceptance that is predicted for NA61 with the upgraded forward tracking (shown in Figure 14).

6.2.3 Design and construction plan

The chambers will be designed, to the extent practical, to take advantage of the existing infrastructure of NA61. There are approximately 200 spare front-end boards, each of which serves 32 individual readout pads. A single motherboard serves 24 front-end boards; therefore the most efficient arrangement of channels is a multiple of 768. We propose to use one motherboard for the upstream chamber and two for the downstream chamber. This puts us well within the limits of the existing spare electronics supply. The drift high voltage supplies used by the other chambers are still in production and can be ordered from the same company.

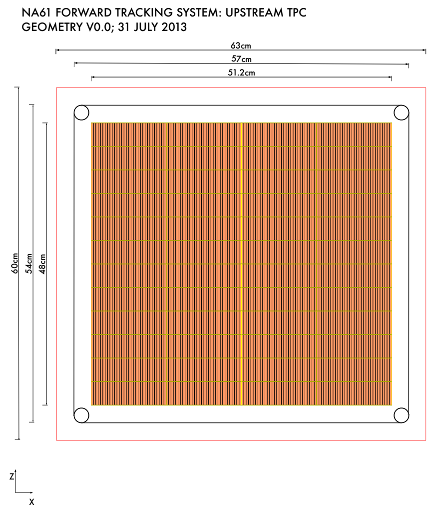

Figure 16: Pad geometry of upstream forward tracking chamber. Yellow lines indicate boundaries between front-end boards; black and red represent respectively the field cage and gas walls.

The planned pad geometry for the upstream chamber is shown in Fig. 16. The arrangement is the same as a single module of the MTPCs, with twelve full rows of 4×40 mm^2 pads. The drift direction will be downward, the opposite of the GTPC and MTPCs. This provides the opportunity to reject out-of-time tracks in tandem with the GTPC, and is also necessary as there is no space for readout cards at the top of the chamber.

The downstream chamber will be a two-cage tandem system. The upstream and downstream pads will be of the normal size, with larger pads in the center in order to maximize dE/dx coverage while minimizing the channel count.

University of Colorado, Boulder is exploring an improvement to the field cage design of the existing chambers, which use a series of individually-clamped aluminized mylar strips that were difficult to assemble. The PHENIX muon arms station 2 detector used an etched mylar sheet to perform a similar function, and we are working with a LANL group that was involved in that effort.

University of Colorado, Boulder is collaborating with the Wigner Institute in Budapest, which has a wire winding machine well suited to our task. They plan to ship the frames and wire to Budapest for winding, and then the completed planes will be transferred to Colorado

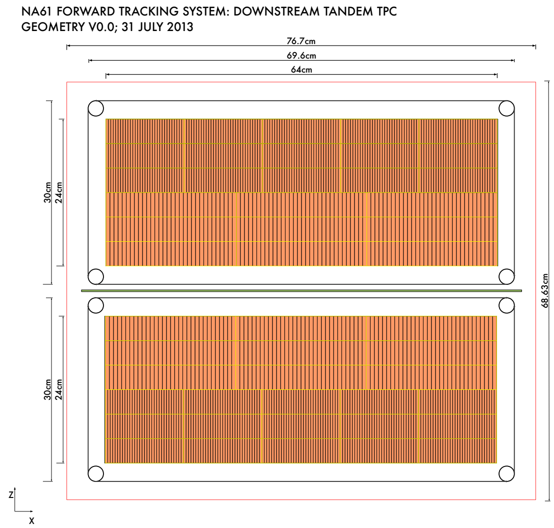

Figure 17: Pad geometry of downstream forward tracking chamber. The two field cages will have electron drift in opposite directions.

for assembly into the chamber. Colorado has the capability to lay out and assemble the boards for the pad planes as well as assemble the full chambers. The chambers' gas system (which will use a simple one-way flow of Ar+CO_2, the same mixture used by the other TPCs in NA61) will be built of standard parts and assembled in place at CERN. We hope to use an existing spare drift velocity monitor.

A proposed schedule for forward tracking follows:

10/2014: Begin mechanical engineering work.

- Wire frame design, including support/fixation within chamber
- Field cage posts, field cage film, and voltage divider
- Outer frame, gas walls, gas connections
- Drift cathode PCB design
- Chamber stand/hanging bracket design

11/2014: CAD models ready

11/2014: Production drawings ready

11/2014: Specify and order drift HV supplies and gas system parts

12/2014: Place orders for custom parts

3/2015: Receive most custom parts

4/2015: Send wire frames to Budapest for winding

6/2015: Received completed frames from Budapest

8/2015: Complete chamber assembly in Boulder

8/2015: Test chambers with cosmic rays in Boulder

10/2015: Transport assembled chambers to CERN

12/2015: Install chambers, gas systems at CERN

2/2016: Ready for beam operation

7 Summary

A major systematic limitation for precision accelerator neutrino experiments is the knowledge of neutrino flux. Past experience has demonstrated that "out of the box" flux modeling does not reproduce the near detector energy spectra. This necessitates the re-weighting of simulated fluxes, however even these procedures do not disentangle the cross-section and the flux calculations. In summary, we propose a program to remedy a long-standing problem in neutrino physics at Fermilab for experiments that use the 120 GeV/c beam, by measuring hadron production at the CERN NA61/SHINE experiment. The data would be relevant for MINERνA, MINOS, MINOS+, and LBNE/LBNF. The program would take about four years to complete. A pilot run, which took place in June 23-24, 2012, has already acquainted US-NA61 collaborators with NA61/SHINE operations and data analysis. By exploiting NA61/SHINE's well developed detector technology and data analysis capabilities, the US-NA61 program is the most cost-effective and timely means of obtaining well understood neutrino beams at Fermilab.

References

[1] D. Drakoulakos *et al.* [Minerva Collaboration], “Proposal to perform a high-statistics neutrino scattering experiment using a fine-grained detector in the NuMI beam,” hep-ex/0405002.

[2] [MINOS+ Collaboration], “A Proposal to FNAL to run MINOS with the medium energy NuMI beam”, Fermilab, May 2011.

[3] D. S. Ayres *et al.* [NOvA Collaboration], “NOvA: Proposal to build a 30 kiloton off-axis detector to study nu(mu) $\rightarrow$ nu(e) oscillations in the NuMI beamline,” hep-ex/0503053.

[4] A. Bravar [NA61/SHINE Collaboration], “Hadro-Production Measurements to Characterize the T2K Neutrino Flux with the NA61 Experiment at the CERN SPS,” AIP Conf. Proc. **1222**, 431 (2010).
C. Strabel [for the NA61/SHINE Collaboration], “Hadro-production measurements for T2K by NA61/SHINE at the CERN SPS,” arXiv:1006.0767 [hep-ex].

[5] K. Abe *et al.* [T2K Collaboration], “The T2K Neutrino Flux Prediction,” Phys. Rev. D **87**, 012001 (2013).

[6] T. Akiri *et al.* [LBNE Collaboration], “The 2010 Interim Report of the Long-Baseline Neutrino Experiment Collaboration Physics Working Groups,” arXiv:1110.6249 [hep-ex].

[7] F. P. An *et al.* [DAYA-BAY Collaboration], “Observation of electron-antineutrino disappearance at Daya Bay,” arXiv:1203.1669 [hep-ex].

[8] Z. Pavlovic, “Observation of Disappearance of Muon Neutrinos in the NuMI Beam,” PhD Thesis, University of Texas Austin, May 2008, FERMILAB-THESIS-2008-59.

[9] L. Fields *et al.* [MINERvA Collaboration], Phys. Rev. Lett. **111**, no. 2, 022501 (2013) [arXiv:1305.2234 [hep-ex]].

[10] N. Abgrall *et al.* [The NA61/SHINE Collaboration], "Measurement of Production Properties of Positively Charged Kaons in Proton-Carbon Interactions at 31 GeV/c", Phys.Rev. C85 (2012) 035210 arXiv:1112.0150 [hep-ex].

[11] "Study of Hadron Production in Hadron-Nucleus and Nucleus-Nucleus Collisions at the CERN-SPS", NA61 Proposal, CERN-SPSC-2006-034, SPSC-P-330.

[12] N. Abgrall *et al.* [NA61/SHINE Collaboration] "NA61/SHINE facility at the CERN SPS: beams and detector system", JINST **9**, P06005 (2014)

[13] G. Ambrosini *et al.* [SPY Collaboration], "Pion yield from 450-GeV/c protons on beryllium," Phys. Lett. B **425**, 208 (1998); G. Ambrosini *et al.* [SPY Collaboration], "K / pi production ratios from 450-GeV/c protons on beryllium," Phys. Lett. B **420**, 225 (1998).

[14] H. W. Atherton *et al.*,, "Precise Measurements of Particle Production by 400 GeV/c Protons on Beryllium Targets", CERN-80-07.

[15] D. S. Barton *et al.*,, "Experimental Study of the A-Dependence of Inclusive Hadron Fragmentation", Phys. Rev. **D27** (1983) 2580.

[16] C. Alt *et al.*, [The NA49 collaboration], "Inclusive production of charged pions in p+C collisions at 158 GeV/c beam momentum", Eur. Phys. J. **C 49**, 897-917 (2007).

[17] A. Bravar [NA61/SHINE Collaboration], "Hadron production measurements for neutrino experiments by the NA61/SHINE experiment at CERN," PoS ICHEP **2010**, 293 (2010); T. J. Palczewski [NA61/SHINE Collaboration], "Pion production measurement in NA61/SHINE experiment," Int. J. Mod. Phys. A **26**, 754 (2011); N. Abgrall *et al.* [NA61/SHINE Collaboration], "Measurements of Cross Sections and Charged Pion Spectra in Proton-Carbon Interactions at 31 GeV/c," Phys. Rev. C **84**, 034604 (2011); N. Abgrall *et al.* [NA61/SHINE Collaboration], "Measurements of Production Properties of K_S^0 mesons and Lambda hyperons in Proton-Carbon Interactions at 31 GeV/c," Phys. Rev. C **89**, 025205 (2014); M. Unger [for the NA61/SHINE Collaboration], "Hadron Production at Fixed Target Energies and Extensive Air Showers," PoS

ICHEP **2010**, 449 (2010); M. Z. Posiadala [NA61/SHINE Collaboration], "Measurements of hadron production for neutrino physics within NA61/SHINE experiment at CERN SPS," Acta Phys. Polon. B **41**, 1585 (2010).

[18] F. Ballarini *et al.*, "The FLUKA code: An overview," J. Phys. Conf. Ser. **41**, 151 (2006); G. Battistoni, F. Broggi, M. Brugger, M. Campanella, M. Carboni, A. Empl, A. Fasso and E. Gadioli *et al.*, "Applications of FLUKA Monte Carlo code for nuclear and accelerator physics," Nucl. Instrum. Meth. B **269**, 2850 (2011).

[19] N. Abgrall *et al.* [The NA61/SHINE Collaboration], "Measurements of Cross Sections and Charged Pion Spectra in Proton-Carbon Interactions at 31 GeV/c". Phys.Rev. C84 (2011) 034604.
N. Abgrall *et al.* [The NA61/SHINE Collaboration], "Pion emission from the T2K replica target: method, results and application", arXiv:1207.2114 [hep-ex].

[20] C. Alt *et al.*, [The NA49 collaboration], "Inclusive production of charged pions in p+p collisions at 158 GeV/c beam momentum", Eur. Phys. J. **C 45**, 343-381 (2006); T. Anticic *et al.*, [The NA49 collaboration], "Inclusive production of charged kaons in p+p collisions at 158 GeV/c beam momentum and a new evaluation of the energy dependence of kaon production up to collider energies", Eur. Phys. J. **C 68**, 1-73 (2010); T. Anticic *et al.*, [The NA49 collaboration], "Inclusive production of protons, anti-protons and neutrons in p+p collisions at 158 GeV/c beam momentum", Eur. Phys. J. **C 65**, 9-63 (2010).

[21] http://www.psi.ch/drs/

[22] N. J. Buchanan, L. Chen, D. M. Gingrich, S. Liu, H. Chen, D. Damazio, F. Densing and S. Duffin *et al.*, "ATLAS liquid argon calorimeter front end electronics," JINST **3**, P09003 (2008).